Journal of Sound and Vibration (2002) **250**(4), 649–673
doi:10.1006/jsvi.2001.3957, available online at http://www.idealibrary.com on IDEAL®

FORCED VIBRATIONS OF TRIPLY COUPLED, PERIODICALLY AND ELASTICALLY SUPPORTED, FINITE, OPEN-SECTION CHANNELS

Y. YAMAN

Department of Aeronautical Engineering, Middle East Technical University, 06531 *Ankara, Turkey*.
E-mails: yyaman@metu.edu.tr, yyaman@ae.metu.edu.tr

AND

Ö. ÖZDEMİR

Tusaş Engine Industries (TEI), Eskişehir, Turkey

(*Received* 1 *June* 2000, *and in final form* 24 *July* 2001)

An exact analytical method is presented for the analysis of forced vibrations of uniform, open-section, single- and multi-bay periodic channels. The centre of gravity and the shear centre of the channel cross-sections do not coincide, and hence the flexural vibrations in two mutually perpendicular directions and the torsional vibrations are all coupled. The ends of the channels and the periodic intermediate supports are modelled with springs having finite flexural and torsional stiffnesses. Single-point force excitation has been considered throughout the study, although the developed method is also capable of dealing with multi-point excitation. The channels are assumed to be of Euler–Bernoulli type beams. The study also takes the effects of cross-sectional warping into consideration. The developed method is suitable for structurally damped analysis and in addition to yielding forced vibration characteristics; it also straightforwardly reveals the free vibration properties like the mode shapes.

1. INTRODUCTION

If the centre of gravity and the shear centre of an open-section channel cross-section do not coincide, the flexural vibrations are inevitably coupled with the torsional vibrations. The stiffener, being an important element of aeronautical structures, is a typical structure, which undergoes such a motion.

Although studies involving finite element methods are numerous in literature, Gere and Lin [1] and Lin [2] presented some of the first analytical works in this field and obtained the coupled, but free vibration characteristics of uniform, open-section channels using the Rayleigh–Ritz method. The effectivenesses of various beam theories in the solution of beams having coupled torsion and bending were compared by Bishop *et al.* [3]. Dokumacı [4] developed an exact analytical model for the determination of coupled vibrations of open-section channels, which were symmetric with respect to an axis, though the warping was not admitted. Bishop *et al.* [5] then allowed warping in Dokumacı's theory and investigated the same type of Euler–Bernoulli beams of open cross-section. In all of these works, only the free vibration characteristics and the classical end boundary conditions were studied. Freiberg developed a numerical method for the solution of coupled beam

0022-460X/02/090649 + 25 $35.00/0

vibrations based on Vlasov theory and obtained the dynamic stiffness matrix [6]. He further established element mass and stiffness matrices for use in standard finite element procedures and evaluated the modal masses. However, he analyzed only the classical end boundary conditions.

Cremer and Heckl [7] proposed a wave propagation method for the solution of forced wave motion in uniform structures. The use of that method was found to be extremely convenient and effective when the responses of finite, uniform structures to point harmonic forces or line harmonic loads were determined [8, 9].

Yaman [10], by using the wave propagation approach, developed exact analytical models for the forced vibration analysis of open-section channels having classical end boundary conditions. In that study, the type of the coupling was defined in terms of the independent motions, which were coupled due to the geometry of cross-sections. Hence if the flexural vibrations in one direction were coupled with torsional vibrations, the resulting phenomenon is called the double coupling; whereas if the flexural vibrations in two mutually perpendicular directions were all coupled with the torsional vibrations, it is referred to as triple coupling. The warping characteristics were also considered but, since they were derived from torsional characteristics and represented through the torsion-bending stiffness, the warping was not treated as an independent motion. The developed theory was able to provide forced vibration characteristics like frequency response curves as well as giving the free vibration properties like the mode shapes. The comparisons showed that the developed method proved to be a good alternative to complicated approaches such as the Vlasov Theory.

If the ends are elastically supported (where the supports may also have inertial properties), the problem becomes very tedious to tackle through the means of the classical analytical approaches. Yaman [11] also developed exact analytical models for the analysis of non-classical end boundary conditions in purely torsional and doubly coupled vibrations of single-bay channels. The exact methods have alleviated the difficulties encountered in the consideration of complex end boundary conditions and proved to be effective. Özdemir studied the dynamics of multi-bay doubly and triply coupled channels [12]. She also considered the periodically supported channels resting on flexible supports.

In references [10–12], the structures were first assumed to be infinite in length and the f1exural and torsional displacements due to the external force and torque excitations were formulated. The displacements due to the waves being reflected from the ends were also separately formulated. The intermediate supports react upon the channel with forces and torques, which generate wave fields similar to those of the externally applied force. The total motion then consists of the wave fields due to the externally applied loading, the intermediate support reactions and the reflections from the extreme ends. The unknowns are the reflected wave amplitudes and the reaction forces and torques due to intermediate supports. Equations for these unknowns are set up by satisfying the boundary conditions at the ends of the finite channel and then by satisfying the compatibility conditions at each support location. Once the unknowns have been determined, the response at any point in the finite channel can be computed. It was found that the developed method, though being primarily intended for the analysis of forced vibrations, was very convenient in the determination of free vibration properties such as the mode shapes. As a matter of fact, any vectorial quantity such as the velocity, acceleration, bending moment or shear force at any point on the channel could easily be obtained.

This study gives the theory and applications for forced, triply coupled vibrations of elastically supported, uniform, open cross-section, single and multi-bay channels. The ends of the channels and the intermediate periodic supports are modelled with springs, which provide finite flexural and torsional stiffnesses. The effects of different end conditions are

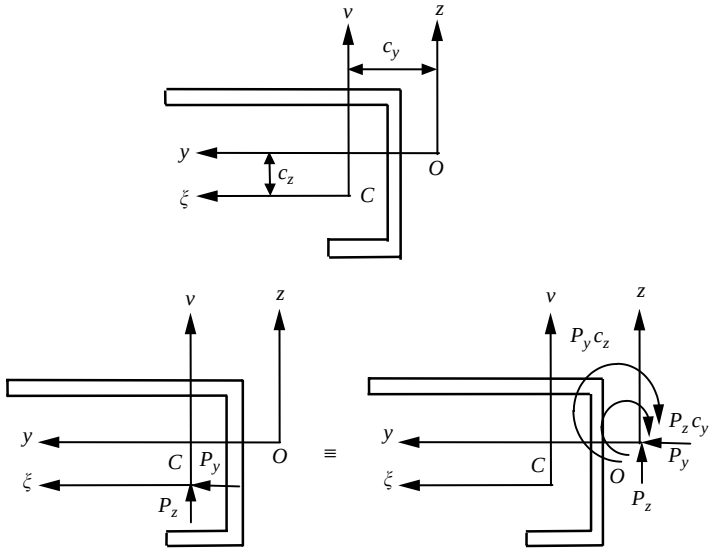

Figure 1. Cross-section representing a triply coupled channel and the real and effective loadings (C: centroid, O: shear centre)

studied. The forcing is taken in the form of a point harmonic load. The effects of warping are also dealt with. Various frequency response curves and the mode shape curves are presented for both undamped and structurally damped channels.

2. THEORY

2.1. THE MOTION GENERATED IN AN INFINITE, TRIPLY COUPLED CHANNEL BY A SINGLE HARMONIC TRANSVERSE FORCE

Consider Figure 1 which gives a typical triply coupled channel, relevant co-ordinate axes and the real and effective loadings. In this case the flexural vibrations in the z direction, flexural vibrations in the y direction and the torsional vibrations are all coupled. The motion equations of this type of coupled vibrations are well known to be [1, 2] (a list of nomenclature is given in Appendix C)

$$EI_\xi \frac{\partial^4 w}{\partial x^4} + m\frac{\partial^2 w}{\partial t^2} + EI_{v\xi}\frac{\partial^4 v}{\partial x^4} + mc_y \frac{\partial^2 \phi}{\partial t^2} = 0,$$

$$EI_v \frac{\partial^4 v}{\partial x^4} + m\frac{\partial^2 v}{\partial t^2} + EI_{v\xi}\frac{\partial^4 w}{\partial x^4} + mc_z \frac{\partial^2 \phi}{\partial t^2} = 0,$$

$$E\Gamma_O \frac{\partial^4 \phi}{\partial x^4} - GJ\frac{\partial^2 \phi}{\partial x^2} + mc_y \frac{\partial^2 w}{\partial t^2} + mc_z \frac{\partial^2 v}{\partial t^2} + \rho I_O \frac{\partial^2 \phi}{\partial t^2} = 0. \tag{1}$$

Here w is the flexural displacement in the z direction, v is the flexural displacement in the y direction and ϕ is the torsional displacement. EI_ξ defines the flexural stiffness in the z direction, EI_v gives the flexural stiffness in the y direction, $EI_{v\xi}$ is the flexural coupling stiffness between the flexural motions in the y and z directions. The centroidal axes v and ξ are not necessarily the principal centroidal axes and the second moments of area I_ξ, I_v and $I_{v\xi}$ are calculated with respect to the centroidal v- and ξ-axis. GJ is the torsional stiffness

and $E\Gamma_O$ is the torsion-bending stiffness with respect to the shear centre O through which the warping characteristics of the cross-section are taken into the consideration. c_y is the eccentricity between the centroid and the shear centre in the y direction, c_z is the eccentricity between the centroid and the shear centre in the z direction, I_O is the second polar moment of area with respect to the shear centre, ρ is the material density and m is the mass per unit length of the uniform channel.

If the torsion-bending stiffness is excluded, 10 coupled waves may travel along the length of the channel and they appear in five positive and negative pairs ($j = 5$), and if one includes the torsion-bending stiffness the number of possible waves becomes 12, in six positive and negative pairs ($j = 6$) [10]. These waves are influenced by both the flexural and the torsional properties of the structure and are characterized by their wave numbers k_n which are the roots of the determinantal equation derived from equations (1). If one considers the existence of the torsion-bending stiffness, the determinantal equation for the wave numbers then becomes

$$\begin{bmatrix} EI_\xi k_n^4 - m\omega^2 & EI_{v\xi} k_n^4 & -mc_y\omega^2 \\ EI_{v\xi} k_n^4 & EI_v k_n^4 - m\omega^2 & -mc_z\omega^2 \\ -mc_y\omega^2 & -mc_z\omega^2 & E\Gamma_O k_n^4 - \rho I_O \omega^2 \end{bmatrix} = 0. \tag{2}$$

The total displacement fields $w(x)$, $v(x)$ and $\phi(x)$, at any point x along the length of the triply coupled channel, have two parts. In each field, the first part is due to the free waves reflected from the left- and right-hand boundaries of the finite channel and the second part is due to the external transverse force(s) as though they were acting on a doubly infinite unrestrained channel. Both of these parts are represented by series expressions. The external transverse forces can be applied in the z direction as P_z and/or in the y direction as P_y.

It has been shown that [10] a single transverse force P_z, when applied alone on the finite channel at x_f through the centroid, and the free waves reflected from the extreme ends will create the following total displacement fields:

$$\begin{aligned} w(x,t) &= \left(\sum_{n=1}^{2j} A_n e^{k_n x} + P_z \sum_{n=1}^{j} a_n e^{-k_n|x-x_f|} \right) e^{i\omega t}, \\ v(x,t) &= \left(\sum_{n=1}^{2j} A_n \Pi_n e^{k_n x} + P_z \sum_{n=1}^{j} a_n \Pi_n e^{-k_n|x-x_f|} \right) e^{i\omega t}, \\ \phi(x,t) &= \left(\sum_{n=1}^{2j} A_n \Phi_n e^{k_n x} + P_z \sum_{n=1}^{j} a_n \Phi_n e^{-k_n|x-x_f|} \right) e^{i\omega t}. \end{aligned} \tag{3}$$

a_n values are found by satisfying the necessary continuity and compatibility conditions at the point of application of P_z acting on a doubly infinite channel. Their determination for the triply coupled channel are given in reference [10]. The A_n values are the unknowns of the problem and represent the complex amplitudes of the $2j$ reflected waves. They are found by satisfying the necessary $2j$ conditions at the ends of the triply coupled channel.

Π_n defines the ratio of the flexural displacement v to the flexural displacement w for an excitation in the z direction (P_z). Similarly, Φ_n gives the ratio of the twist ϕ to the flexural displacement w, for P_z excitation. They can be found from equation (1) as

$$\begin{aligned} \Pi_n &= \frac{(EI_\xi k_n^4 - m\omega^2)(E\Gamma_O k_n^4 - GJk_n^2 - \rho I_O \omega^2) - (-c_y m\omega^2)^2}{(-c_y m\omega^2)(-c_z m\omega^2) - (EI_{v\xi} k_n^4)(E\Gamma_O k_n^4 - GJk_n^2 - \rho I_O \omega^2)}, \\ \Phi_n &= \frac{(EI_\xi k_n^4 - m\omega^2)\ (EI_v k_n^4 - m\omega^2) - (EI_{v\xi} k_n^4)^2}{(EI_{v\xi} k_n^4)\ (-c_z m\omega^2) - (-c_y m\omega^2)\ (EI_v k_n^4 - m\omega^2)}. \end{aligned} \tag{4}$$

If required, the warping displacement can also be found from the torsional displacement as

$$u(x,t) = -2As\frac{\partial\phi(x,t)}{\partial x} = -2As\left(\sum_{n=1}^{2j} k_n A_n \Phi_n e^{k_n x} - P_z \sum_{n=1}^{j} k_n a_n \Phi_n e^{-k_n|x-x_f|}\right)e^{i\omega t}, \quad (5)$$

where As is the swept area.

2.2. THE BOUNDARY CONDITIONS TO BE SATISFIED AT THE ENDS OF AN ELASTICALLY SUPPORTED TRIPLY COUPLED CHANNEL

The development of boundary conditions for classically supported ends of triply coupled channels is given in reference [10] in detail. Similarly, the boundary conditions for elastically supported ends of the doubly coupled channel vibrations are given in reference [11]. This study extends those theories and gives the end conditions for elastically supported and triply coupled channels. Upon assuming no rotational restraint to exist in both xy and xz planes, the following set of equations (6)–(9) gives the required boundary conditions for the case where both ends warp freely.

Relations due to flexural springs, K_t:

$$\begin{aligned}&(EI_\xi w'''(0) + EI_{v\xi} v'''(0)) + K_{tw,l} w(0) = 0, \quad (EI_\xi w'''(L) + EI_{v\xi} v'''(L))\\ &\quad - K_{tw,r}\, w(L) = 0, \quad (EI_v v'''(0) + EI_{v\xi} w'''(0)) + K_{tv,l} v(0) = 0,\\ &(EI_v v'''(L) + EI_{v\xi} w'''(L)) - K_{tv,r} v(L) = 0, \end{aligned} \quad (6)$$

where $K_{tw,l}$ and $K_{tw,r}$ are the transverse flexural stiffnesses resisting w displacements at the left- and right-hand ends respectively. $K_{tv,l}$ and $K_{tv,r}$ are those which resist the corresponding v displacements, and L is the length of the channel.

Rotational relations where the channel is free to rotate in both xz and xy planes:

$$w''(0) = 0, \quad w''(L) = 0, \quad v''(0) = 0, \quad v''(L) = 0. \quad (7)$$

Relations due to torsional springs, K_{tor}:

$$(GJ\phi'(x) - E\Gamma_O\phi'''(x))|_{x=0} - K_{tor,l}\phi(0) = 0, \quad (GJ\phi'(x) - E\Gamma_O\phi'''(x))|_{x=L} + K_{tor,r}\phi(L) = 0, \quad (8)$$

where $K_{tor,l}$ and $K_{tor,r}$ are the torsional stiffnesses resisting ϕ displacements at the left- and right-hand ends respectively.

End warping relations:

$$u'(0) = 0,\ u'(L) = 0 \quad \text{(i.e., } \phi''(0) = 0 \text{ and } \phi''(L) = 0). \quad (9)$$

When the expressions for w, v, ϕ and u from equations (3) and (5) are substituted into equations (6)–(9), one obtains a matrix equation for the unknown A_n's as

$$[C_{SB}]\{A_n\} = -P_z\{D_{SB}\}, \quad (10)$$

where SB stands for single-bay. The numerical solution of equation (10) yields the required unknowns, A_n's. Their further substitution into equations (3) and (5) allows one to determine the required displacements at any point on the channel.

Expressions for the coefficients of C_{SB} and D_{SB} of equation (10) are given in Appendix A in detail.

2.3. THE INFLUENCE OF AN INTERMEDIATE ELASTIC SUPPPORT

Now consider the effects of an intermediate elastic support located at $x = x_m$ which restrains both the twisting rotation and the w and v flexural displacements. Denote the support stiffness which resists twist by $K_{s,tor}$ and those which resist displacements w and v by $K_{st,w}$ and $K_{st,v}$ respectively. The torque exerted on the channel by the support is therefore $T_m = -K_{s,tor}\phi(x_m)$ and the forces exerted on the channel are $Rz_m = -K_{st,w}w(x_m)$ and $Ry_m = -K_{st,v}v(x_m)$. Each of these unknown forces and the torque create different flexural displacements and twist at any point on the channel. These fields are similar in form to those created by an externally applied force (i.e., equations (3)) but have different coefficients. The total displacement fields $w(x)$, $v(x)$ and $\phi(x)$ due to the combined effect of those unknown forces and torque can be found to be

$$w(x) = \left(\sum_{m=1}^{k} R_{z_m} \sum_{n=1}^{j} a_n e^{-k_n|x-x_m|} + \sum_{m=1}^{k} T_m \sum_{n=1}^{j} \psi_n b_n e^{-k_n|x-x_m|} + \sum_{m=1}^{k} R_{y_m} \sum_{n=1}^{j} \gamma_n c_n e^{-k_n|x-x_m|} \right),$$

$$v(x) = \left(\sum_{m=1}^{k} R_{z_m} \sum_{n=1}^{j} \Pi_n a_n e^{-k_n|x-x_m|} + \sum_{m=1}^{k} T_m \sum_{n=1}^{j} \lambda_n b_n e^{-k_n|x-x_m|} + \sum_{m=1}^{k} R_{y_m} \sum_{n=1}^{j} c_n e^{-k_n|x-x_m|} \right),$$

$$\varphi(x) = \left(\sum_{m=1}^{k} R_{z_m} \sum_{n=1}^{j} \Phi_n a_n e^{-k_n|x-x_m|} + \sum_{m=1}^{k} T_m \sum_{n=1}^{j} b_n e^{-k_n|x-x_m|} + \sum_{m=1}^{k} R_{y_m} \sum_{n=1}^{j} \sigma_n c_n e^{-k_n|x-x_m|} \right), \tag{11}$$

where k defines the number of intermediate supports. The coefficients Π_n and Φ_n are those given in equation (4). ψ_n relates the flexural displacement w to the unknown torque T_m. γ_n relates the flexural displacement w to the unknown force applied in the y direction, Ry_m. λ_n gives the relation between the flexural displacement v and the unknown torque T_m. Similarly, σ_n defines the relation between the twist ϕ and the unknown force Ry_m. By using equations (1) and (4), these coefficients can be found to be

$$\lambda_n = \frac{(EI_\xi k_n^4 - m\omega^2)(m\omega^2 c_z) - (m\omega^2 c_y)(EI_{v\xi} k_n^4)}{(EI_v k_n^4 - m\omega^2)(EI_\xi k_n^4 - m\omega^2) - (EI_{v\xi} k_n^4)^2}, \quad \gamma_n = 1/\Pi_n, \quad \sigma_n = 1/\lambda_n, \quad \psi_n = 1/\Phi_n. \tag{12}$$

b_n values in equation (11) are obtained from the following continuity and compatibility conditions satisfied at the point of application of a torque T, as if it were acting on a doubly infinite channel:

$$EI_\xi \frac{\partial^3 w(x,t)}{\partial x^3} + EI_{v\xi} \frac{\partial^3 v(x,t)}{\partial x^3} = 0, \quad \frac{\partial w(x,t)}{\partial x} = 0,$$

$$EI_v \frac{\partial^3 v(x,t)}{\partial x^3} + EI_{v\xi} \frac{\partial^3 w(x,t)}{\partial x^3} = 0, \quad \frac{\partial v(x,t)}{\partial x} = 0,$$

$$GJ \frac{\partial \phi(x)}{\partial x} - E\Gamma_o \frac{\partial^3 \phi(x)}{\partial x^3} = -\frac{T}{2}, \quad u(x,t) = \frac{\partial \phi(x,t)}{\partial x} = 0. \tag{13}$$

Substituting the T-dependent terms of equations (11) into these equations, one obtains the following set of equations for the b_n's:

$$EI_\xi \sum_{n=1}^{j} -k_n^3 \psi_n b_n + EI_{v\xi} \sum_{n=1}^{j} -k_n^3 \lambda_n b_n = 0, \quad EI_v \sum_{n=1}^{j} -k_n^3 \lambda_n b_n + EI_{v\xi} \sum_{n=1}^{j} -k_n^3 \psi_n b_n = 0,$$

$$GJ\sum_{n=1}^{j} - k_n b_n - E\Gamma_{\mathrm{O}}\sum_{n=1}^{j} - k_n^3 b_n = -T/2, \quad \sum_{n=1}^{j} - k_n^3\psi_n b_n = 0, \quad \sum_{n=1}^{j} - k_n^3\lambda_n b_n = 0,$$

$$\sum_{n=1}^{j} - k_n b_n = 0. \tag{14}$$

These equations can further be put in a general matrix form of order j as

$$[X_T]\{b_n\} = -\{x_T\}, \tag{15}$$

where T stands for Torque and the coefficients of X_T in row-wise order become

$$X_{T_{1,n}} = -EI_\xi k_n^3\psi_n - EI_{v\xi}k_n^3\lambda_n, \quad X_{T_{2,n}} = -EI_v k_n^3\lambda_n - EI_{v\xi}k_n^3\psi_n,$$

$$X_{T_{3,n}} = -GJk_n - E\Gamma_{\mathrm{O}}(-k_n^3), \quad X_{T_{4,n}} = -k_n^3\psi_n, \quad X_{T_{5,n}} = -k_n^3\lambda_n, \quad X_{T_{6,n}} = -k_n, \tag{16}$$

where in each row the index n varies from 1 to j ($j = 6$). The forcing vector is given by

$$\{x_T\}^{\mathrm{T}} = \{0\ 0\ -T/2\ 0\ 0\ 0\}. \tag{17}$$

The numerical solution of equation (15) yields the required b_n values.

The c_n values in equation (11) can be found by a similar process. When a transverse load P_y acts on a doubly infinite channel in the y direction, the following continuity and compatibility conditions must be satisfied at the location of the load P_y:

$$EI_\xi\frac{\partial^3 w(x,t)}{\partial x^3} + EI_{v\xi}\frac{\partial^3 v(x,t)}{\partial x^3} = 0, \quad \frac{\partial w(x,t)}{\partial x} = 0,$$

$$EI_v\frac{\partial^3 v(x,t)}{\partial x^3} + EI_{v\xi}\frac{\partial^3 w(x,t)}{\partial x^3} = \frac{P_y}{2}, \quad \frac{\partial v(x,t)}{\partial x} = 0,$$

$$GJ\frac{\partial\phi(x,t)}{\partial x} - E\Gamma_{\mathrm{O}}\frac{\partial^3\phi}{\partial x^3} = \frac{P_y c_z}{2}, \quad u(x,t) = \left.\frac{\partial\phi(x,t)}{\partial x}\right|_{x=0} = 0. \tag{18}$$

Substituting into these equations the R_y-dependent terms of equation (11), one obtains the following matrix equation for the c_n's:

$$[X_{PY}]\{c_n\} = -\{x_{PY}\}. \tag{19}$$

The coefficients of X_{PY} can be given in a row-wise order as

$$X_{PY_{1,n}} = -EI_\xi k_n^3\gamma_n - EI_{v\xi}k_n^3, \quad X_{PY_{2,n}} = -EI_v k_n^3 - EI_{v\xi}k_n^3\gamma_n,$$

$$X_{PY_{3,n}} = -GJk_n\sigma_n - E\Gamma_{\mathrm{O}}(-k_n^3)\sigma_n, \quad X_{PY_{4,n}} = -k_n^3\gamma_n, \quad X_{PY_{5,n}} = -k_n^3, \quad X_{PY_{6,n}} = -k_n\sigma_n, \tag{20}$$

where in each row, n varies between 1 and j ($j = 6$) and the forcing vector is given by

$$\{x_{PY}\}^T = \{0\ \ P_y/2\ \ (P_y c_z)/2\ \ 0\ \ 0\ \ 0\}.$$

The required c_n values are computed from the numerical solution of equation (19).

Now on the multi-bay channel, each of the k sets of those unknown reaction forces Rz_m, Ry_m and the unknown reaction torque T_m create displacements w, v and ϕ. The externally applied force (only P_z in this case) and the amplitudes A_n of the waves reflected from the

extreme ends also create displacement fields. By combining the effects of all those, the total displacement fields $w(x)$, $v(x)$, $\phi(x)$ in a triply coupled channel can then be written as

$$w(x,t) = \Bigg(\sum_{n=1}^{2j} A_n e^{k_n x} + P_z \sum_{n=1}^{j} a_n e^{-k_n|x-x_f|} + \sum_{m=1}^{k} R_{z_m} \sum_{n=1}^{j} a_n e^{-k_n|x-x_m|} + \sum_{m=1}^{k} T_m \sum_{n=1}^{j} \psi_n b_n e^{-k_n|x-x_m|} + \sum_{m=1}^{k} R_{y_m} \sum_{n=1}^{j} \gamma_n c_n e^{-k_n|x-x_m|} \Bigg) e^{i\omega t},$$

$$v(x,t) = \Bigg(\sum_{n=1}^{2j} \Pi_n A_n e^{k_n x} + P_z \sum_{n=1}^{j} \Pi_n a_n e^{-k_n|x-x_f|} + \sum_{m=1}^{k} R_{z_m} \sum_{n=1}^{j} \Pi_n a_n e^{-k_n|x-x_m|} + \sum_{m=1}^{k} T_m \sum_{n=1}^{j} \lambda_n b_n e^{-k_n|x-x_m|} + \sum_{m=1}^{k} R_{y_m} \sum_{n=1}^{j} c_n e^{-k_n|x-x_m|} \Bigg) e^{i\omega t},$$

$$\varphi(x,t) = \Bigg(\sum_{n=1}^{2j} \Phi_n A_n e^{k_n x} + P_z \sum_{n=1}^{j} \Phi_n a_n e^{-k_n|x-x_f|} + \sum_{m=1}^{k} R_{z_m} \sum_{n=1}^{j} \Phi_n a_n e^{-k_n|x-x_m|} + \sum_{m=1}^{k} T_m \sum_{n=1}^{j} b_n e^{-k_n|x-x_m|} + \sum_{m=1}^{k} R_{y_m} \sum_{n=1}^{j} \sigma_n c_n e^{-k_n|x-x_m|} \Bigg) e^{i\omega t}. \tag{21}$$

The unknown reaction forces Rz_m, Ry_m and the reaction torque T_m should satisfy the compatibility conditions at each support location x_m. In this way, it can be written that

$$w(x_m) = -Rz_m/K_{st,w}, \qquad v(x_m) = -Ry_m/K_{st,v}, \qquad \phi(x_m) = -T_m/K_{s,\,tor}. \tag{22}$$

The support at x_m is assumed to be symmetric, in that there is no stiffness coupling between the three prescribed displacements of the supports (i.e., an imposed force on the support in one direction does not induce displacements in either of the other directions). Each of the support stiffnesses may be different and furthermore may include the effects of support inertia.

Consider a support at $x = x_s$. Substituting the expressions for $w(x_s)$, $v(x_s)$ and $\phi(x_s)$ from equations (21) into equations (22) and then rearranging the equation, one obtains the following three equations for the unknown A_n's and R's:

$$\Bigg(\sum_{n=1}^{2j} A_n e^{k_n x_s} + P_z \sum_{n=1}^{j} a_n e^{-k_n|x_s-x_f|} + \sum_{m=1\ \text{to}\ k,\ m\neq s} R_{z_m} \sum_{n=1}^{j} a_n e^{-k_n|x_s-x_m|} + R_{z_s} \Bigg(\sum_{n=1}^{j} a_n + (1/K_{st,w}) \Bigg) + \sum_{m=1}^{k} T_m \sum_{n=1}^{j} \psi_n b_n e^{-k_n|x_s-x_m|} + \sum_{m=1}^{k} R_{y_m} \sum_{n=1}^{j} \gamma_n c_n e^{-k_n|x_s-x_m|} \Bigg) = 0, \tag{23}$$

$$\Bigg(\sum_{n=1}^{2j} \Pi_n A_n e^{k_n x_s} + P_z \sum_{n=1}^{j} \Pi_n a_n e^{-k_n|x_s-x_f|} + \sum_{m=1}^{k} R_{z_m} \sum_{n=1}^{j} \Pi_n a_n e^{-k_n|x_s-x_m|} + \sum_{m=1}^{k} T_m \sum_{n=1}^{j} \lambda_n b_n e^{-k_n|x_s-x_m|} + \sum_{m=1\ \text{to}\ k,\ m\neq s} R_{y_m} \sum_{n=1}^{j} c_n e^{-k_n|x_s-x_m|} + R_{y_s} \Bigg(\sum_{n=1}^{j} c_n + (1/K_{st,v}) \Bigg) \Bigg) = 0, \tag{24}$$

$$\left(\sum_{n=1}^{2j} \Phi_n A_n e^{k_n x_s} + P_z \sum_{n=1}^{j} \Phi_n a_n e^{-k_n|x_s - x_f|} \right.$$

$$+ \sum_{m=1}^{k} R_{z_m} \sum_{n=1}^{j} \Phi_n a_n e^{-k_n|x_s - x_m|} + \sum_{m=1 \text{ to } k,\, m \neq s} T_m \sum_{n=1}^{j} b_n e^{-k_n|x_s - x_m|}$$

$$\left. + T_s \left(\sum_{n=1}^{j} b_n + (1/K_{s,\,tor}) \right) + \sum_{m=1}^{k} R_{y_m} \sum_{n=1}^{j} \sigma_n c_n e^{-k_n|x_s - x_m|} \right) = 0. \tag{25}$$

In this way, three equations can be found for each intermediate support location. The k intermediate supports therefore yield $3k$ such equations. The boundary conditions at the extreme ends of the elastically supported channel together yield another $2j$ equations for the $2j$ unknown A_n's ($j = 5$ or 6 depending on the inclusion of torsion-bending stiffness $E\Gamma_O$). The total set of $3k + 2j$ equations is sufficient to allow all the unknowns of the problem to be determined. If P_z is the only external force acting on the system, the relevant set of equations has the following matrix form:

$$[C_{MB}]\{X\} = -P_z\{D_{MB}\}, \tag{26}$$

where MB stands for multi-bay and

$$\{X\}^T = \{A_1 \;\; A_2 \;\; \ldots \;\; A_n \;\; R_{z_1} \;\; R_{z_2} \;\; \ldots \;\; R_{z_k} \;\; R_{y_1} \;\; \ldots \;\; R_{y_k} \;\; T_1 \;\; \ldots \;\; T_k\}.$$

C_{MB} values are the coefficients of unknowns for continuity and the compatibility conditions satisfied at the extreme ends and at each intermediate support location. D_{MB} values are the coefficients of the externally applied loading P_z for continuity and the compatibility conditions satisfied at the extreme ends and at each intermediate support location. The expressions for the terms of equation (26) are given in Appendix B.

The required A_n, Rz_k, Ry_k and T_k values are numerically found from equation (26). Their substitution into equations (21) yields the required $w(x)$, $v(x)$ and $\phi(x)$ displacements at any point on the elastically supported, periodic channel.

If the torsion-bending stiffness $E\Gamma_O$ is excluded from the analysis, j becomes 5. Hence, the terms involving $E\Gamma_O$ and ϕ'' should appropriately be deleted from the relevant equations.

If the externally applied transverse force is in the y direction as P_y or a combination of P_z and P_y, then all the equations starting from equation (3) should be modified by considering the relevant theory given in reference [10]. Here it is worth mentioning that despite these modifications, the order of the resulting matrix equation will not change. The required changes will take place only at the right-hand side of equations, the forcing vector.

3. RESULTS AND DISCUSSION

This section presents the computed results, frequency responses and the non-dimensional normalized mode shapes of the single- and multi-bay, elastically and periodically supported triply coupled channels.

The force excitation is in the form of a point harmonic force $P_z e^{i\omega t}$. The frequency responses are computed as receptances (displacement/force). The point of the application of the force is taken as $x_f = 0{\cdot}13579$ m and the flexural responses are determined at the same point. This rather strange point is selected in order to avoid any possible nodes. Structural damping is included through the complex flexural stiffnesses as $EI_\xi^* = EI_\xi(1 + i\eta_\xi)$, $EI_v^* = EI_v(1 + i\eta_v)$ and $EI_{v\xi}^* = EI_{v\xi}(1 + i\eta_{v\xi})$ and through the complex torsional stiffness as $GJ^* = GJ(l + i\eta_t)$. To calculate natural frequencies, resonance frequencies were found for

the system with very light damping ($\eta_\xi = \eta_v = \eta_{v\xi} = \eta_t = 10^{-6}$). The resonance frequencies were carefully identified by zooming in on the frequencies which yielded maximum harmonic response. The systems considered were the single-bay channel and periodically supported channels with either two, three or four bays. The bay lengths of the multi-bay channels were all the same as the span of the single-bay channel. The effects of including or excluding torsion-bending stiffness and flexural coupling stiffness as well as the effects of changing the stiffnesses of the elastic supports have been studied.

The channel cross-section is given in Figure 1. The material and geometrical properties of the channels considered are as follows:

$A = 9{\cdot}68 \times 10^{-5}$ m^2, $I_v = 5{\cdot}08 \times 10^{-9}$ m^4, $I_\xi = 2{\cdot}24 \times 10^{-8}$ m^4, $I_{v\xi} = 4{\cdot}25 \times 10^{-9}$ m^4, $c_y = 10{\cdot}43 \times 10^{-3}$ m, $c_z = 9{\cdot}09 \times 10^{-3}$ m, $J = 5{\cdot}20 \times 10^{-11}$ m^3, $I_O = 4{\cdot}60 \times 10^{-8}$ m^4, $\rho = 2700$ kg/m^3, $E = 7 \times 10^{10}$ N/m^2, $G = 2{\cdot}6 \times 10^{10}$ N/m^2, $\Gamma_O = 2{\cdot}334 \times 10^{-11}$ m^6, $XL = 1$ m, $L = nXL$ where L is the total length of the channels, XL is the periodic bay length of the channels and n is the bay number.

3.1. NATURAL FREQUENCIES OF A SIMPLY SUPPORTED, SINGLE-BAY CHANNEL

In this section, first the proposed model is validated, by considering a single-bay channel with elastically supported ends. Both ends of the channel are assigned the same spring stiffness values of $K_{t,w} = K_{t,v} = 10^{20}$ N/m and $K_{tor} = 10^{20}$ Nm. This case corresponds to a simply supported, triply coupled channel for which the relevant resonance frequency data is available [10]. Table 1 gives the first seven resonance frequencies for the cases in which the effects of the torsion-bending stiffness $E\Gamma_O$ and flexural coupling stiffness $EI_{v\xi}$ are excluded and included in turn.

The results are exactly the same as those previously obtained in reference [10] from classical end conditions. It can further be seen that the effects of including the torsion-bending stiffness increases all of the resonance frequencies, not just the torsional frequencies. This is a consequence of the coupling between torsion and flexure. It can also be seen that the inclusion of flexural coupling stiffness has a greater effect when the torsion-bending stiffness is also included. The results show clearly that the torsion-bending stiffness and flexural coupling stiffness must both be included if accurate frequencies are to be determined.

TABLE 1

Effects of $E\Gamma_O$ and $EI_{v\xi}$ on the resonance frequencies (Hz) *of the single-bay, triply coupled channel* ($K_{t,w} = K_{t,v} = 10^{20}$ (N/m), $K_{tor} = 10^{20}$ (N m), $\eta_\xi = \eta_v = \eta_{v\xi} = \eta_t = 10^{-06}$)

$E\Gamma_O = 0$		$E\Gamma_O$ included	
$EI_{v\xi} = 0$	$EI_{v\xi}$ included	$EI_{v\xi} = 0$	$EI_{v\xi}$ included
45·489	45·311	57·451	51·866
69·909	60·317	115·079	114·795
101·731	102·209	229·667	207·413
149·817	155·178	259·006	263·786
154·848	159·939	458·443	456·586
207·447	207·695	516·689	466·657
257·292	220·026	918·519	829·598

TABLE 2

Uncoupled resonance frequencies (Hz) *of the single-bay, triply coupled channel* ($K_{t,w} = K_{t,v} = 10^{20}$ (N/m), $K_{tor} = 10^{20}$ (N m), $\eta_\xi = \eta_v = \eta_{v\xi} = \eta_t = 10^{-06}$)

Flexural		Torsional	
Flexure in y	Flexure in z	$E\Gamma_O = 0$	$E\Gamma_O$ included
57·969	121·846	52·165	187·491
231·876	487·383	104·331	727·866
521·720	1096·612	156·496	1628·326
927·502	1949·532	208·662	2888·947

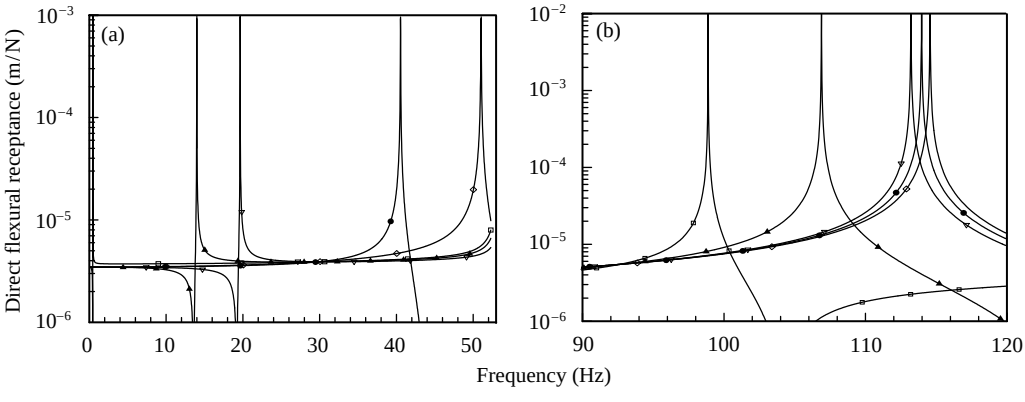

Figure 2. Effects of K_{tor} on the resonance frequencies of the single-bay channel ($K_{t,w} = K_{t,v} = 10^{20}$ N/m, $\eta_\xi = \eta_v = \eta_{v\xi} = \eta_t = 10^{-6}$, $E\Gamma_O$ and $EI_{v\xi}$ included: (a) –□–, $K_{tor} = 5 \times 10^{-4}$ N m; –▲–, $K_{tor} = 5 \times 10^{-1}$ N m;–▽–, $K_{tor} = 1 \times 10^{0}$ N m; –●–, $K_{tor} = 5 \times 10^{0}$ N m; –◇–, $K_{tor} = 5 \times 10^{2}$ N m; (b) –□–, $K_{tor} = 5 \times 10^{1}$ N m; –▲–, $K_{tor} = 1 \times 10^{2}$ N m; –▽–, $K_{tor} = 5 \times 10^{2}$ N m; –●–, $K_{tor} = 1 \times 10^{3}$ N m; –◇–, $K_{tor} = 5 \times 10^{3}$ N m).

The first four uncoupled flexural resonance frequencies of the channel for $K_{t,w} = 10^{20}$ N/m, $K_{t,v} = 10^{20}$ N/m and $K_{tor} = 10^{20}$ Nm are presented in Table 2 for comparison with the coupled resonance frequencies of Table 1. Table 2 also gives the uncoupled torsional resonance frequencies for the cases where torsion-bending stiffness $E\Gamma_O$ is either included or not and indicates the important effects of $E\Gamma_O$.

3.2. THE EFFECTS OF RELAXING THE SUPPORT STIFFNESSES ON THE RESONANCE FREQUENCIES OF SINGLE-BAY, TRIPLY COUPLED CHANNELS

The effects of the spring stiffness values on the resonance frequencies of an elastically supported single-bay channel are now considered.

In this context, first the effects of the torsional stiffness K_{tor} are studied. Both ends of the channel are assumed to be supported by $K_{t,w} = 10^{20}$ N/m and $K_{t,v} = 10^{20}$ N/m and K_{tor} values are varied. The torsion-bending stiffness $E\Gamma_O$ and the flexural coupling stiffness $EI_{v\xi}$ are both taken into consideration. The resulting frequency response curves are shown in Figure 2(a) and 2(b) for the first two resonance frequencies of the single-bay, triply coupled channel respectively. It can be seen from Figure 2(a) that when K_{tor} values are low, the resonance frequency goes to zero, the frequency of the rigid-body torsional mode. As the K_{tor} values increase the resonance frequency approaches 51·866 Hz. Further increase in

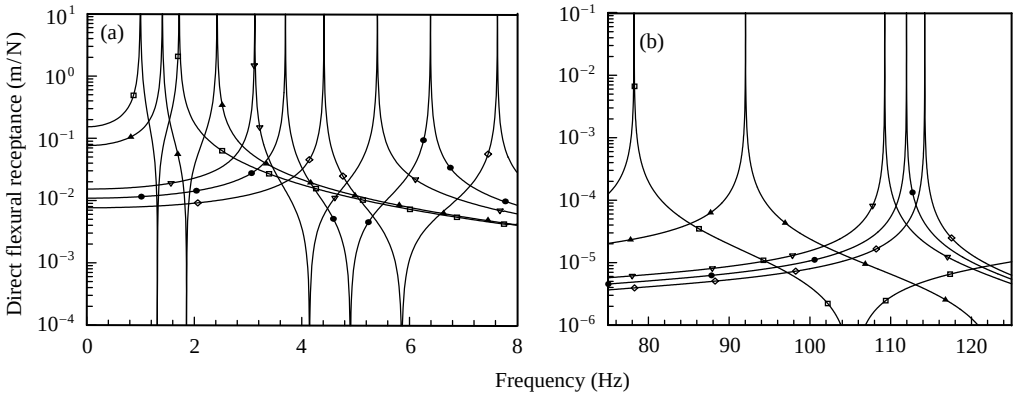

Figure 3. Effects of $K_{t,w}$ on the resonance frequencies of the single-bay channel ($K_{t,v} = 10^{20}$ N/m; $K_{tor} = 10^{20}$ N m; $\eta_\xi = \eta_v = \eta_{v\xi} = \eta_t = 10^{-6}$, $E\Gamma_O$ and $EI_{v\xi}$ included: (a) –□–, $K_{t,w} = 5 \times 10^0$ N/m; –▲–, $K_{t,w} = 1 \times 10^1$ N/m; –▽–, $K_{t,w} = 5 \times 10^1$ N/m; –●–, $K_{t,w} = 7 \times 10^1$ N/m; –◇–, $K_{t,w} = 1 \times 10^2$ N/m; (b) –□–, $K_{t,w} = 5 \times 10^4$ N/m; –▲–, $K_{t,w} = 1 \times 10^5$ N/m; –▽–, $K_{t,w} = 5 \times 10^5$ N/m; –●–, $K_{t,w} = 1 \times 10^6$ N/m; –◇–, $K_{t,w} = 5 \times 10^6$ N/m).

K_{tor} also affects the higher frequencies and as shown in Figure 2(b), the second resonance frequency approaches 114·795 Hz. After a certain K_{tor} is achieved, any more increase does not appreciably affect the resonance frequencies.

In order to analyze the effects of the transverse spring support stiffness, $K_{t,w}$ has been varied ($K_{t,w}$ restrains z-wise flexural motion) while the other support stiffnesses have been held at the very high values of $K_{t,v} = 10^{20}$ N/m and $K_{tor} = 10^{20}$ Nm. As $K_{t,w}$ approaches zero, the resonance frequency also approaches zero which is the frequency of both the rigid-body z-wise vertical translation mode and the rigid-body pure rotational mode in the plane of the structure. As $K_{t,w}$ assumes non-zero but very small values, the structure also undergoes a vertical translation mode and pure rotational mode at very low frequencies. At very low values of $K_{t,w}$, the lowest resonance frequency is that of a mode involving predominantly z-wise displacement. Figure 3(a) represents this case, for low $K_{t,w}$ values, as double peaks in the response curves for a very low-frequency range of 0–8 Hz. In each curve, the first peak corresponds to the vertical translation mode in the z direction and the second peak represents the pure rotational mode in the xz plane. Figure 3(b) shows that as $K_{t,w}$ increases indefinitely, the lowest frequency of the triply coupled channel approaches the asymptotic value of 51·866 Hz, while the second frequency approaches 114·795 Hz.

Further calculations have demonstrated that the effects of changing $K_{t,v}$ on resonance frequencies are generally similar to those of changing $K_{t,w}$. This is true whether or not $E\Gamma_O$ and/or $EI_{v\xi}$ are included.

3.3. RESONANCE FREQUENCIES AND FREQUENCY RESPONSE CURVES OF PERIODIC CHANNELS

The resonance frequencies of the channels are presented next. Single-bay and two-, three -and four-bay periodic channels are studied. Periodic channels have bays of the same length as the single-bay beam, which has already been studied. Both ends of the periodic channels are supported by springs having $K_{t,w} = K_{t,v} = 10^{20}$ N/m, $K_{tor} = 10^{20}$ Nm. The intermediate support stiffnesses are also assigned to $K_{st,w} = K_{st,v} = 10^{20}$ N/m and

TABLE 3

Bounding frequencies (Hz) *of the propagation zones of the triply coupled channel* ($\eta_\xi = \eta_v = \eta_{v\xi} = \eta_t = 10^{-06}$)

	$E\Gamma_O = 0$		$E\Gamma_O$ included	
Zone	$EI_{v\xi} = 0$	$EI_{v\xi}$ included	$EI_{v\xi} = 0$	$EI_{v\xi}$ included
1	45·489–51·198	45·311–51·383	57·451–130·157	51·866–117·546
2	69·909–103·363	60·317–103·558	115·079–259·822	114·795–258·634
3	101·731–143·119	102·209–123·915	229·667–358·743	207·413–324·005
4	149·817–157·591	155·178–156·007	259·006–572·362	263·786–583·850
5	154·848–207·571	159·939–207·776	458·443–703·249	456·586–635·166
6	207·447–259·927	207·695–260·091	516·689–715·641	466·657–712·449
7	257·292–312·168	220·026–312·238	918·519–1162·481	829·598–1049·952

$K_{s,tor} = 10^{20}$ Nm. This corresponds to simply supported ends and intermediate simple supports.

It is well known from the periodic structures theory that the resonance frequencies of an n-bay periodic structure occur in groups of n and these groups also occur within certain frequency bands. The zones in which the resonance frequencies do occur and which are identified by the bounding frequencies are called the propagation zones. The nth lower bounding frequency of each propagation zone actually corresponds to the nth resonance frequency of the single-bay structure with simply supported ends and the nth upper bounding frequency of each propagation zone can be identified as the nth resonance frequency of the single-bay structure with clamped ends [8, 9].

Table 3 gives the bounding frequencies of all the cases considered in the study for the first seven corresponding propagation zones. For each case, the lower bounding frequency of the nth zone was determined to be the nth simply supported resonance frequency of the single-bay, triply coupled channel and similarly the upper bounding frequency of the nth zone was computed to be the nth clamped–clamped resonance frequency of the same single-bay channel. For the cases in which the torsion-bending stiffness was taken into consideration, the clamped natural frequencies were found by assuming no axial displacement (i.e., warping displacement) at the ends although the axial displacement was allowed everywhere else in the channel. It can be seen that in all the cases presented, some of the zones do overlap while some of them do not. The frequency zones between the separate propagation zones are known as the attenuation zones and in these zones, wave propagation is not possible. For example, in Table 3 the attenuation zones of the case, where the torsion-bending stiffness and the flexural coupling stiffness are not included in the analysis, are from 51·198 to 69·909 Hz and from 143·119 to 149·817 Hz. The other attenuation zones can likewise be identified in all the cases given. The presence of attenuation zones within the covered frequency range indicates that in triply coupled channels, the wave propagation takes place in a wide range of frequencies but not at all frequencies.

Now consider a beam with intermediate simple supports, and either with simply supported ends or the clamped ends. It is known that [8, 9] if the ends are simply supported, the first resonance frequency of the nth zone is equal to the nth resonance frequency of the simply supported, single-bay channel and furthermore if the ends are clamped the nth resonance frequency of the nth zone is equal to the nth resonance frequency of the clamped–clamped, single-bay channel. The remaining $(n - 1)$ resonance frequencies of each

TABLE 4

Effects of end conditions on the resonance frequencies (Hz) *of the two-bay, triply coupled channel* ($K_{st,w} = K_{st,v} = 10^{20}$ (N/m), $K_{s,tor} = 10^{20}$ (N m), $\eta_\xi = \eta_v = \eta_{v\xi} = \eta_t = 10^{-06}$, $E\Gamma_O$ *and* $EI_{v\xi}$ *included*)

Propagation zone	Simply supported	Ends Clamped	Ends
1	51·866	81·329	117·546
2	114·795	178·148	258·634
3	207·413	262·496	324·005

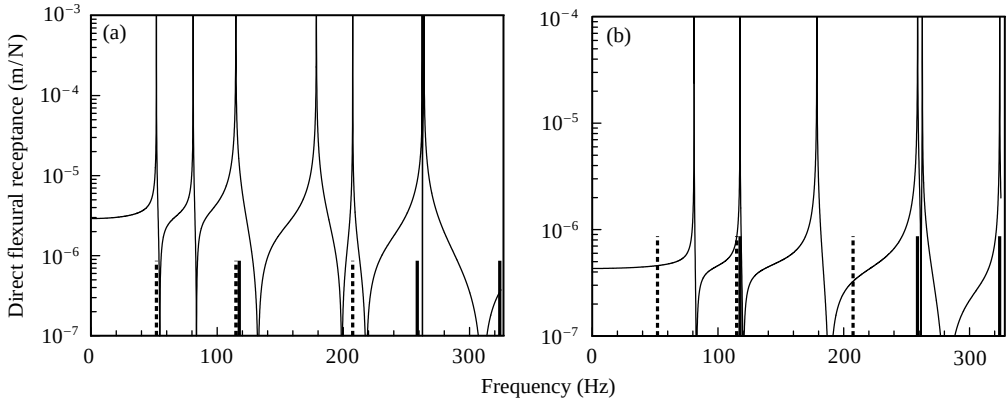

Figure 4. Effects of end conditions on the resonance frequencies of the two-bay channel having intermediate support ($K_{st,w} = 10^{20}$ N/m, $K_{st,v} = 10^{20}$ N/m, $K_{s,tor} = 10^{20}$ N m, $\eta_\xi = \eta_v = \eta_{v\xi} = \eta_t = 10^{-6}$, $E\Gamma_O$ and $EI_{v\xi}$ included: (a) both ends simply supported; (b) both ends clamped: - - - lines define the beginnings and — lines define the ends of the first three propagation zones).

zone are identical for both cases. The same characteristic has also been observed in triply coupled channels and given in Table 4 for the two-bay channel where the flexural coupling stiffness $EI_{v\xi}$ and the torsion-bending stiffness $E\Gamma_O$ are all taken into consideration. Figure 4(a) and 4(b), on the other hand, shows the frequency responses for the simply supported ends and clamped ends respectively. The beginning and end of each propagation zone are also indicated as vertical lines in Figure 4(a) and 4(b). Consideration of Figure 4(a) and Table 3 shows that, due to the overlapping propagation zones, the resonance frequency of 263·786 Hz, which is in fact the lower bounding frequency of the fourth propagation zone, also appears in the frequency response.

The results for periodic channels are now presented. In order to show their impacts on the resonance frequencies of the periodic channels, $EI_{v\xi}$ and $E\Gamma_O$ are first excluded from the analysis. The corresponding resonance frequencies of all four channels having bay numbers from one to four are shown in Table 5 for a range including the first three resonance frequencies of the single-bay channel, which actually corresponds to the first three propagation zones. The results for the case where $EI_{v\xi}$ and $E\Gamma_O$ are all considered, are given in Table 6 for the same spring stiffness values of Table 5 and again for the first three resonance frequencies of the corresponding single-bay channel. Both Tables 5 and 6 show that the second resonance frequencies of the two-bay channels are identical to the third resonance frequencies of the four-bay channels.

TABLE 5

Effects of number of bays on the resonance frequencies (Hz) *of the triply coupled periodic channel* ($K_{t,w} = K_{t,v} = 10^{20}$ (N/m), $K_{tor} = 10^{20}$ (N m), $K_{st,w} = 10^{20}$ (N/m), $K_{st,v} = 10^{20}$ (N/m), $K_{s,tor} = 10^{20}$ (N m), $\eta_\xi = \eta_v = \eta_{v\xi} = \eta_t = 10^{-06}$, $E\Gamma_O = 0$, $EI_{v\xi} = 0$)

	One-bay	Two-bay	Three-bay	Four-bay
First resonance	45·489	45·489	45·489	45·489
		49·989	48·622	47·668
			50·733	49·989
				50·949
Second resonance	69·909	69·909	69·909	69·909
		97·994	84·695	78·495
			101·291	97·994
				101·547
Third resonance	101·731	101·731	101·731	101·731
		106·471	103·452	103·286
			121·535	106·471
				129·93

TABLE 6

Effects of number of bays on the resonance frequencies (Hz) *of the triply coupled periodic channel* ($K_{t,w} = K_{t,v} = 10^{20}$ (N/m), $K_{tor} = 10^{20}$ (N m), $K_{st,w} = 10^{20}$ (N/m), $K_{st,v} = 10^{20}$ (N/m), $K_{s,tor} = 10^{20}$ (N m), $\eta_\xi = \eta_v = \eta_{v\xi} = \eta_t = 10^{-06}$, $E\Gamma_O$ *and* $EI_{v\xi}$ *included*)

	One-bay	Two-bay	Three-bay	Four-bay
First resonance	51·866	51·866	51·866	51·866
		81·329	66·672	60·519
			97·058	81·329
				104·610
Second resonance	114·795	114·795	114·795	114·795
		178·148	146·659	133·631
			214·315	178·148
				225·147
Third resonance	207·413	207·413	207·413	207·413
		262·496	236·374	230·416
			290·087	262·496
				302·822

Figure 5(a) and 5(b) shows the frequency responses of the four-bay channels for the cases where $EI_{v\xi}$ and $E\Gamma_O$ are either all excluded from the analysis or all included. Since the bounding frequencies are increased by the stiffening effect of torsion-bending stiffness; in a given frequency range there are fewer resonances with $E\Gamma_O$ than without it. Figure 5(a) and 5(b), respectively, shows the frequency responses for a frequency range of 40–140 Hz and indeed covers the first three propagation zones of the four-bay channel with no torsion-bending stiffness and no flexural coupling stiffness. It can be seen that, for the structure considered, this stiffening effect is prominent even at low frequencies.

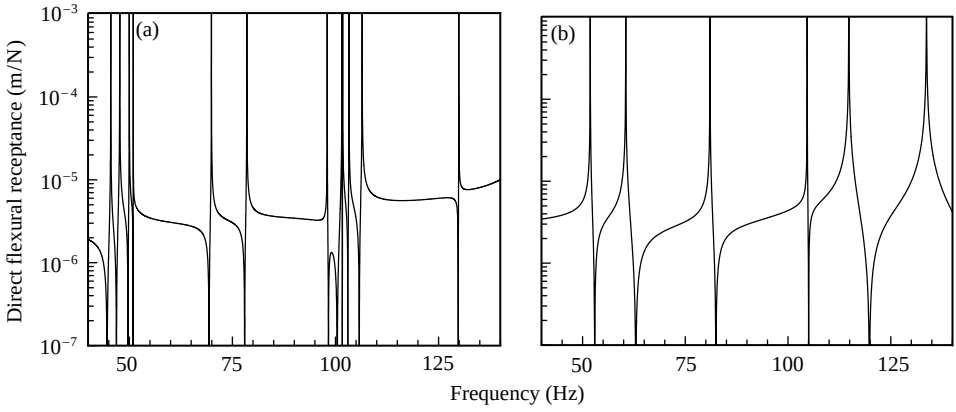

Figure 5. Effects of $E\Gamma_O$ and $EI_{v\xi}$ on the resonance frequencies of the four-bay periodic channel ($K_{t,w} = 10^{20}$ N/m, $K_{t,v} = 10^{20}$ N/m; $K_{tor} = 10^{20}$ N m, $K_{st,w} = 10^{20}$ N/m, $K_{st,v} = 10^{20}$ N/m, $K_{s,tor} = 10^{20}$ N m, $\eta_\xi = \eta_v = \eta_{v\xi} = \eta_t = 10^{-6}$: (a) $E\Gamma_O = 0$ and $EI_{v\xi} = 0$; (b) $E\Gamma_O$ and $EI_{v\xi}$ included).

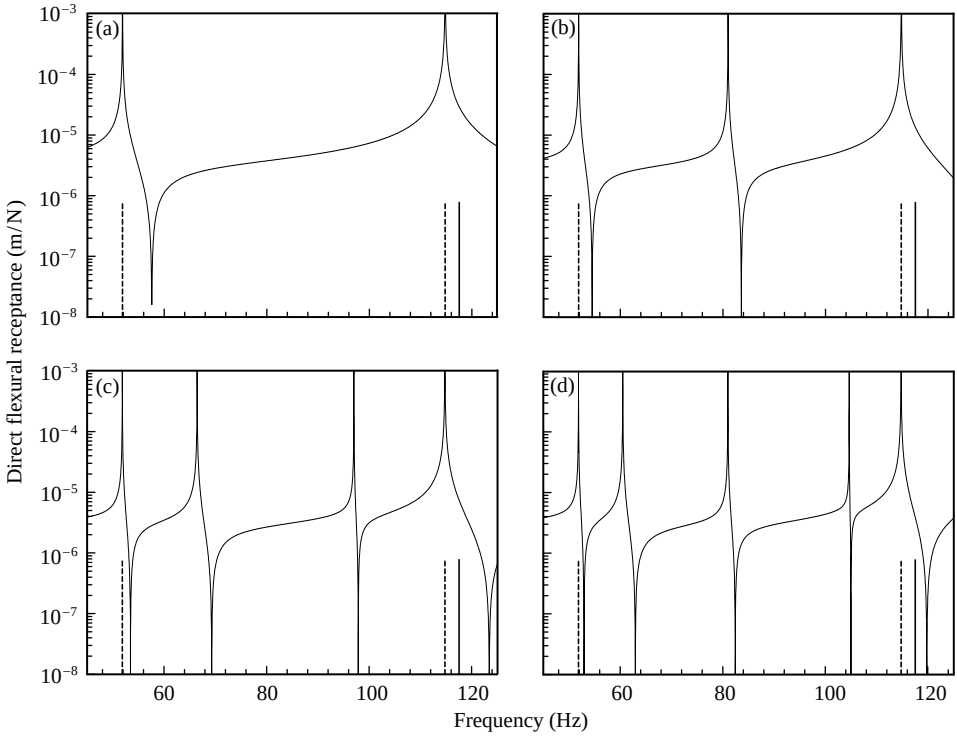

Figure 6. Effects of number of bays on the resonance frequencies of the four-bay periodic channel ($K_{t,w} = 10^{20}$ N/m, $K_{t,v} = 10^{20}$ N/m, $K_{tor} = 10^{20}$ N m, $K_{st,w} = 10^{20}$ N/m, $K_{st,v} = 10^{20}$ N/m, $K_{s,tor} = 10^{20}$ N m, $\eta_\xi = \eta_v = \eta_{v\xi} = \eta_t = 10^{-6}$, $E\Gamma_O$ and $EI_{v\xi}$ included. (a) single-bay, (b) two-bay, (c) three-bay, (d) four-bay: - - - lines define the beginnings and — lines define the ends of the propagation zones).

Figure 6 illustrates the effects of number of bays on the resonance frequencies of the multi-bay periodic channels. Figure 6(a)–6(d) represents the frequency response of one- to four-bay periodic channels in turn. The $E\Gamma_O$ and $EI_{v\xi}$ are included in the analysis. The peaks are the first group of resonance frequencies given in Table 6. Each curve has a peak at

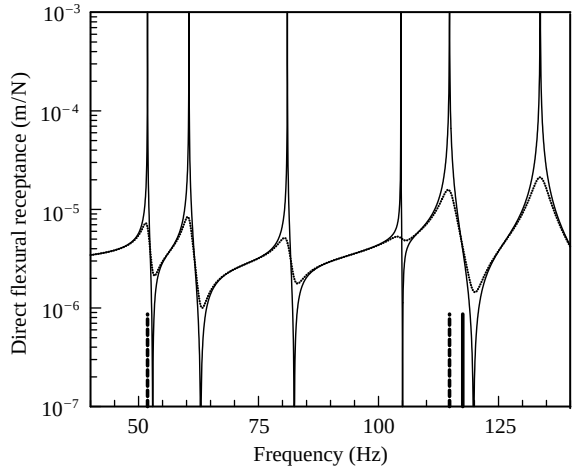

Figure 7. Effects of damping on the resonance frequencies of the four-bay periodic channel ($K_{t,w} = 10^{20}$ N/m, $K_{t,v} = 10^{20}$ N/m, $K_{tor} = 10^{20}$ N m, $K_{st,w} = 10^{20}$ N/m, $K_{st,v} = 10^{20}$ N/m, $K_{s,tor} = 10^{20}$ N m, $E\Gamma_O$ and $EI_{v\xi}$ included: —— $\eta_\xi = \eta_v = \eta_{v\xi} = \eta_t = 0{\cdot}03$, - - - $\eta_\xi = \eta_v = \eta_{v\xi} = \eta_t = 0{\cdot}03$, - - - lines define the beginnings and — lines define the ends of the propagation zones.

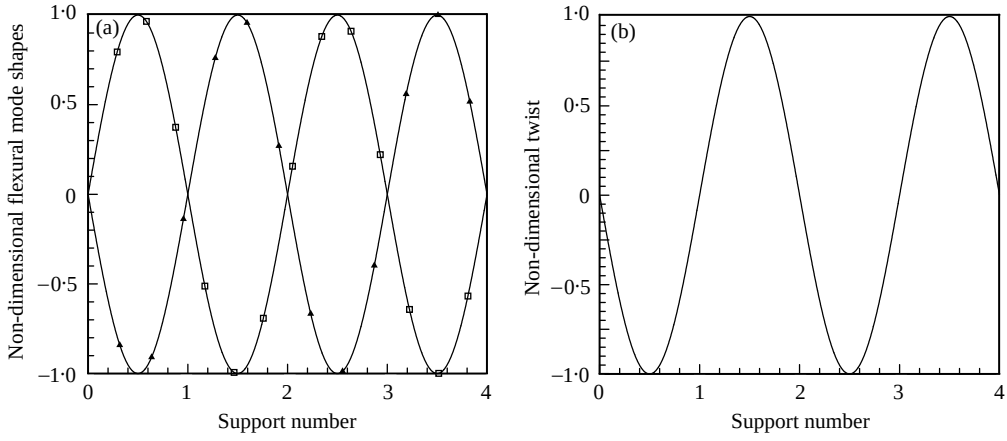

Figure 8. Non-dimensional first mode shapes of the four-bay periodic channel ($K_{t,w} = 10^{20}$ N/m, $K_{t,v} = 10^{20}$ N/m, $K_{tor} = 10^{20}$ N m, $K_{st,w} = 10^{20}$ N/m, $K_{st,v} = 10^{20}$ N/m, $K_{s,tor} = 10^{20}$ N m, $E\Gamma_O$ and $EI_{v\xi}$ included: $f = 51{\cdot}866$ Hz, $\eta_\xi = \eta_v = \eta_{v\xi} = \eta_t = 0$, (a) flexural: –□–, in z direction; –▲–, in y direction; (b) torsional).

51·866 Hz which is the lower bounding frequency of the first propagation zone and at 114·795 Hz which is the lower bounding frequency of the second propagation zone. The upper bounding frequency of the first propagation zone of the channels is also indicated in the figures.

Figure 7 shows the effects of damping on the frequency response of the four-bay periodic channel, which was previously considered and given in Figure 5(b). Two different damping coefficients of 10^{-6} and 0·03 are studied and the corresponding frequency responses are shown in Figure 7. It can be seen that, as expected, the damping is effective only at the resonance and anti-resonance regions.

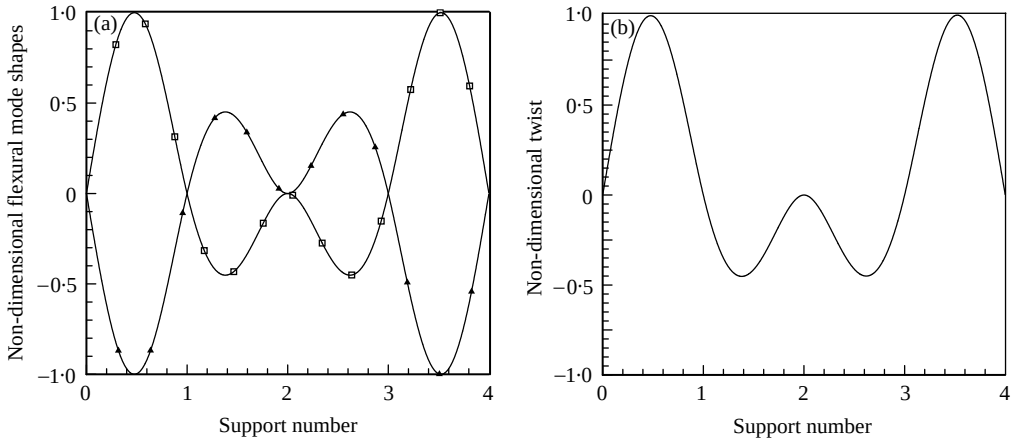

Figure 9. Non-dimensional second mode shapes of the four-bay periodic channel ($K_{t,w} = 10^{20}$ N/m, $K_{t,v} = 10^{20}$ N/m, $K_{tor} = 10^{20}$ N m, $K_{st,w} = 10^{20}$ N/m, $K_{st,v} = 10^{20}$ N/m, $K_{s,tor} = 10^{20}$ N m, $E\Gamma_O$ and $EI_{v\xi}$ included: $f = 60{\cdot}519$ Hz, $\eta_\xi = \eta_v = \eta_{v\xi} = \eta_t = 0$, (a) flexural –□–, in z direction; –▲–, in y direction; (b) torsional).

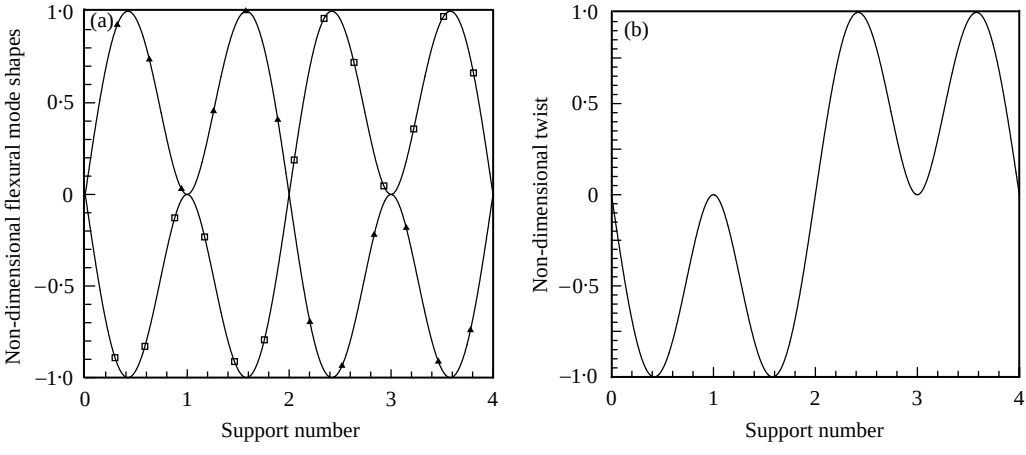

Figure 10. Non-dimensional third mode shapes of the four-bay periodic channel ($K_{t,w} = 10^{20}$ N/m, $K_{t,v} = 10^{20}$ N/m, $K_{tor} = 10^{20}$ N m, $K_{st,w} = 10^{20}$ N/m, $K_{st,v} = 10^{20}$ N/m, $K_{s,tor} = 10^{20}$ N m, $E\Gamma_O$ and $EI_{v\xi}$ included: $f = 81{\cdot}329$ Hz, $\eta_\xi = \eta_v = \eta_{v\xi} = \eta_t = 0$, (a) flexural: –□–, in z direction, –▲–, in y direction; (b) torsional).

3.4. MODES OF VIBRATION OF THE FOUR-BAY PERIODIC CHANNEL

Figures 8–11 give the undamped, non-dimensional flexural and torsional mode shapes of the four-bay periodic channel at the frequencies of 51·866, 60·519, 81·329 and 104·610 Hz. These are the resonance frequencies in the first propagation zone of the four-bay, periodic channel when $EI_{v\xi}$ and $E\Gamma_O$ are included in the analysis and are also given in Table 6. Figures 8(a)–11(a) represent the flexural mode shapes in the z and y directions and Figures 8(b)–11(b) give the variation of twist along the length of the channels. The figures show the capability of the developed method to yield the free vibration properties as well.

4. CONCLUSIONS

In this study, the triply coupled vibrations of single and multi-bay open-section channels are analyzed for a variety of support conditions. It is found that in triply coupled vibrations

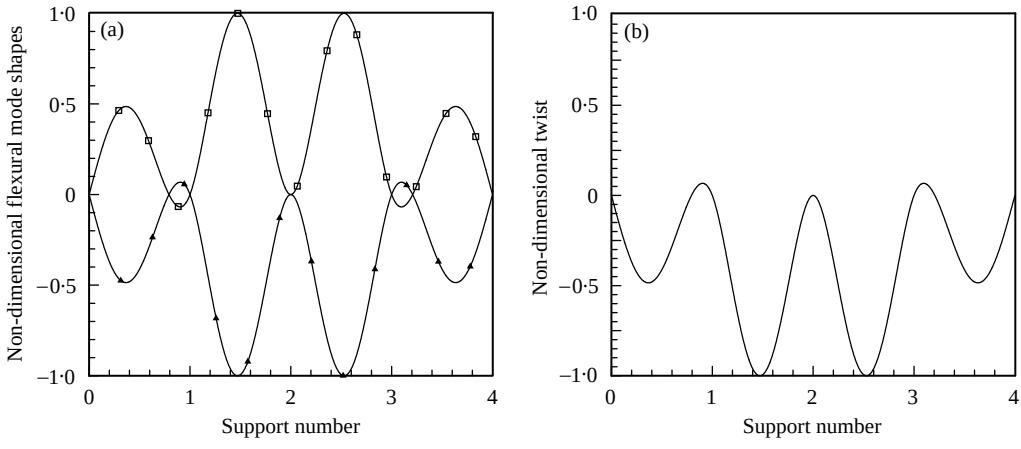

Figure 11. Non-dimensional fourth mode shapes of the four-bay periodic channel ($K_{t,w} = 10^{20}$ N/m, $K_{t,v} = 10^{20}$ N/m, $K_{tor} = 10^{20}$ N m, $K_{st,w} = 10^{20}$ N/m, $K_{st,v} = 10^{20}$ N/m, $K_{s,tor} = 10^{20}$ N m, $E\Gamma_O$ and $EI_{v\xi}$ included: $f = 104{\cdot}610$ Hz, $\eta_\xi = \eta_v = \eta_{v\xi} = \eta_t = 0$, (a) flexural: –□–, in z direction; –▲–, in y direction, (b) torsional).

both the torsional and flexural stiffnesses of the supports are influential. They, because of the coupling, affect all the flexural and torsional modes. Increase in the support stiffnesses values leads to increase in all the resonance frequencies. These results, which are widely known for uncoupled vibrations, were also determined to be similar for the channels, which underwent the doubly coupled vibrations and had elastic supports [11].

It was determined that due to the existing coupling mechanisms, in triply coupled channels the wave propagation takes place in a wide range of frequencies, but not at all frequencies. The wave propagation range is found to be wider if the torsion-bending stiffness is taken into consideration. Due to the existing coupling mechanisms; the regularly alternating attenuation and propagation zones, which is a common feature of independent vibrations, are determined not to appear and some overlapping of the zones occurred.

The developed analytical method, which is found to yield exact results for complicated end conditions, is also capable of analyzing the response due to multi-point and/or distributed loadings. This can simply be achieved by modifying the terms of the forcing vector without increasing the order of the relevant matrix equation. The method presented can also be used in the forced and/or free vibration analysis of uniform open-section channels that are supported non-periodically and/or by any type of support. On the other hand, the present model does not take the effects of the cross-sectional distortion of the channel flanges into consideration, a phenomenon which will be important at very high frequencies.

REFERENCES

1. J. M. Gere and Y. K. Lin 1958 *Journal of Applied Mechanics, Transactions of the American Society of Mechanical Engineers* **80**, 373–378. Coupled vibrations of thin-walled beams of open cross-section.
2. Y. K. Lin 1960 *Journal of Applied Mechanics, Transactions of the American Society of Mechanical Engineers* **82**, 739–740. Coupled vibrations of restrained thin-walled beams.
3. R. E. D. Bishop, W. G. Price and Z. Xi-Cheng 1985 *Journal of Sound and Vibration* **99**, 155–167. A note on the dynamical behaviour of uniform beams having open channel section.
4. E. Dokumaci 1987 *Journal of Sound and Vibration* **119**, 443–449. An exact solution for coupled bending and torsion vibrations of uniform beams having single cross-sectional symmetry.

5. R. E. D. BISHOP, S. M. CANNON and S. MIAO 1989 *Journal of Sound and Vibration* **131**, 457–464. On coupled bending and torsional vibration of uniform beams.
6. P. O. FREIBERG 1985 *International Journal for Numerical Methods in Engineering* **21**, 1205–1228. Beam element matrices derived from Vlasov's theory of open thin-walled elastic beams.
7. L. CREMER and M. HECKL 1988 *Structure-Borne Sound*. Berlin: Springer-Verlag.
8. Y. YAMAN 1989 *Ph.D. Thesis, University of Southampton, England*. Wave receptance analysis of vibrating beams and stiffened plates.
9. D. J. MEAD and Y. YAMAN 1990 *Journal of Sound and Vibration* **141**, 465–484. The harmonic response of uniform beams on multiple linear supports: a flexural wave analysis.
10. Y. YAMAN 1997 *Journal of Sound and Vibration* **204**, 131–158. Vibrations of open-section channels: a coupled flexural and torsional wave analysis.
11. Y. YAMAN 1997 *Proceedings of the 6th International Conference on Recent Advances in Structural Dynamics, University of Southampton, England*. Analytical modelling of coupled vibrations of elastically supported channels.
12. Ö. ÖZDEMİR 1998 *M.Sc. Thesis, Middle East Technical University, Ankara, Turkey*. Forced, coupled vibrations of beams.

APPENDIX A: MATRIX EQUATION FOR ELASTICALLY SUPPORTED SINGLE-BAY CHANNEL

Appendix A gives the terms of matrix equation (10), which is repeated here for convenience.

$$[C_{SB}]\{A_n\} = -P_z\{D_{SB}\}, \tag{A1}$$

where *SB* stands for single-bay. In the construction of equation (A1), equations (6)–(9) are applied in the order given in section 2.

The following set gives the elements of matrix C_{SB} in row-wise order, for the case where the torsion-bending stiffness $EI_{\Gamma O}$ is included in the analysis ($j = 6$). The index n varies from 1 to $2j$, and hence 12 row expressions are given. The expressions in the terms are defined in section 2.

$$C_{SB_{1,n}} = (EI_\xi k_n^3 + EI_{v\xi} k_n^3 \Pi_n + K_{tw,l}), \quad C_{SB_{2,n}} = (EI_\xi k_n^3 e^{k_n L} + EI_{v\xi} k_n^3 \Pi_n e^{k_n L} - K_{tw,r} e^{k_n L}),$$

$$C_{SB_{3,n}} = (EI_v k_n^3 \Pi_n + EI_{v\xi} k_n^3 + K_{tv,l} \Pi_n), \quad C_{SB_{4,n}} = (EI_v k_n^3 \Pi_n e^{k_n L} + EI_{v\xi} k_n^3 e^{k_n L} - K_{tv,r} \Pi_n e^{k_n L}),$$

$$C_{SB_{5,n}} = k_n^2, \quad C_{SB_{6,n}} = k_n^2 e^{k_n L}, \quad C_{SB_{7,n}} = k_n^2 \Pi_n, \quad C_{SB_{8,n}} = k_n^2 \Pi_n e^{knL},$$

$$C_{SB_{9,n}} = (GJk_n \Phi_n - EI_{\Gamma O} k_n^3 \Phi_n - K_{tor,l} \Phi_n),$$

$$C_{SB_{10,n}} = (GJk_n \Phi_n e^{k_n L} - EI_{\Gamma O} k_n^3 \Phi_n e^{k_n L} + K_{tor,r} \Phi_n e^{k_n L}), \quad C_{SB_{11,n}} = k_n^2 \Phi_n, \quad C_{SB_{12,n}} = k_n^2 \Phi_n e^{k_n L}. \tag{A2}$$

If one excludes the torsion-bending stiffness, the required C_{SB} values are the 10×10 upper-left part of matrix C_{SB} given in equation (A1). The terms involving torsion-bending stiffness $EI_{\Gamma O}$ should also be deleted from the ninth and 10th rows of equation (A2).

The following set of equations gives the elements of forcing vector D_{SB} for the case where the torsion-bending stiffness is included in the analysis. Since $j = 6$, there are 12 terms:

$$D_{SB_1} = \left((-1) EI_\xi \sum_{n=1}^{j} - k_n^3 a_n e^{-k_n |x_f|} + (-1) EI_{v\xi} \sum_{n=1}^{j} - k_n^3 \Pi_n a_n e^{-k_n |x_f|} + K_{tw,l} \sum_{n=1}^{j} a_n e^{-k_n |x_f|} \right),$$

$$D_{SB_2} = \left(EI_\xi \sum_{n=1}^{j} - k_n^3 a_n e^{-k_n |L - x_f|} + EI_{v\xi} \sum_{n=1}^{j} - k_n^3 \Pi_n a_n e^{-k_n |L - x_f|} + K_{tw,r} \sum_{n=1}^{j} a_n e^{-k_n |L - x_f|} \right),$$

$$D_{SB_3} = \left((-1)EI_v \sum_{n=1}^{j} -k_n^3 \Pi_n a_n e^{-k_n|x_f|} + (-1)EI_{v\xi} \sum_{n=1}^{j} -k_n^3 a_n e^{-k_n|x_f|} + K_{tv,l} \sum_{n=1}^{j} \Pi_n a_n e^{-k_n|x_f|} \right),$$

$$D_{SB_4} = \left(EI_v \sum_{n=1}^{j} -k_n^3 \Pi_n a_n e^{-k_n|L-x_f|} + EI_{v\xi} \sum_{n=1}^{j} -k_n^3 a_n e^{-k_n|L-x_f|} - K_{tv,r} \sum_{n=1}^{j} \Pi_n a_n e^{-k_n|L-x_f|} \right),$$

$$D_{SB_5} = \left(\sum_{n=1}^{j} k_n^2 a_n e^{-k_n|x_f|} \right), \quad D_{SB_6} = \left(\sum_{n=1}^{j} k_n^2 a_n e^{-k_n|L-x_f|} \right),$$

$$D_{SB_7} = \left(\sum_{n=1}^{j} k_n^2 \Pi_n a_n e^{-k_n|x_f|} \right), \quad D_{SB_8} = \left(\sum_{n=1}^{j} k_n^2 \Pi_n a_n e^{-k_n|L-x_f|} \right),$$

$$D_{SB_9} = \left((-1)GJ \sum_{n=1}^{j} -k_n \Phi_n a_n e^{-k_n|x_f|} - (-1)E\Gamma_O \sum_{n=1}^{j} -k_n^3 \Phi_n a_n e^{-k_n|x_f|} - K_{tor,l} \sum_{n=1}^{j} \Phi_n a_n e^{-k_n|x_f|} \right),$$

$$D_{SB_{10}} = \left(GJ \sum_{n=1}^{j} -k_n \Phi_n a_n e^{-k_n|L-x_f|} - E\Gamma_O \sum_{n=1}^{j} -k_n^3 \Phi_n a_n e^{-k_n|L-x_f|} + K_{tor,r} \sum_{n=1}^{j} \Phi_n a_n e^{-k_n|L-x_f|} \right),$$

$$D_{SB_{11}} = \left(\sum_{n=1}^{j} k_n^2 \Phi_n a_n e^{-k_n|x_f|} \right), \quad D_{SB_{12}} = \left(\sum_{n=1}^{j} k_n^2 \Phi_n a_n e^{-k_n|L-x_f|} \right). \tag{A3}$$

The shear force and the torque expressions are antisymmetric with respect to the point of application of a transverse force (here P_z). Since the terms D_{SB1}, D_{SB3}, and D_{SB9} are representing the boundary conditions at the left-hand side of the applied transverse force P_z, for taking the effects of antisymmetry into consideration, (-1) values are included.

If the torsion-bending stiffness is excluded from the analysis, the required D_{SB} values are the first 10 elements of vector D_{SB} given in equation (A3), provided that the terms involving $E\Gamma_O$ at the elements D_{SB9} and D_{SB10} are omitted.

APPENDIX B: MATRIX EQUATION FOR ELASTICALLY SUPPORTED MULTI-BAY, PERIODIC CHANNEL

Appendix B gives the terms of matrix equation (26), which is repeated here for convenience:

$$[C_{MB}]\{X\} = -P_z\{D_{MB}\}, \tag{B1}$$

where MB stands for multi-bay.

The matrix C_{MB} can further be partitioned as

$$\begin{bmatrix} [A] & [B] \\ [E] & [G] \end{bmatrix}. \tag{B2}$$

For any j ($j = 5$ or 6) value, matrix A is the same as matrix C_{MB} given in Appendix A.

The following equations give the coefficients of matrix B which is $2j \times 3k$ in order. The elements are given in row-wise order, for the case where the torsion-bending stiffness is included ($j = 6$) in the analysis. The expressions in the terms have been previously defined in section 2:

$$B_{1,n1} = R_{z_m}\left((-1)EI_\xi \sum_{n=1}^{j} -k_n^3 a_n e^{-k_n|x_m|} + (-1)EI_{v\xi} \sum_{n=1}^{j} -k_n^3 \Pi_n a_n e^{-k_n|x_m|} + K_{tw,l} \sum_{n=1}^{j} a_n e^{-k_n|x_m|} \right),$$

$$B_{1,n2} = R_{y_m}\left((-1)EI_\xi \sum_{n=1}^{j} -k_n^3 \gamma_n c_n e^{-k_n|x_m|} + (-1)EI_{v\xi} \sum_{n=1}^{j} -k_n^3 c_n e^{-k_n|x_m|} + K_{tw,l} \sum_{n=1}^{j} \gamma_n c_n e^{-k_n|x_m|} \right)$$

$$B_{1,n3} = T_m\Bigg((-1)EI_\xi \sum_{n=1}^{j} -k_n^3 \Psi_n b_n \mathrm{e}^{-k_n|x_m|} + (-1)EI_{v\xi} \sum_{n=1}^{j} -k_n^3 \lambda_n b_n \mathrm{e}^{-k_n|x_m|} + K_{tw,l} \sum_{n=1}^{j} \Psi_n b_n \mathrm{e}^{-k_n|x_m|}\Bigg).$$

In the designation of unknown reaction forces Rz_m and Ry_m and unknown torque T_m, the index m varies from 1 to k where k defines the number of intermediate supports. Furthermore, in each row the column index assumes different ranges. $n1$ varies from 1 to k, $n2$ takes the values between $k+1$ and $2k$ and $n3$ assumes the values from $2k+1$ to $3k$. Effectively, each group varies from 1 to k within its range.

The shear force expressions are antisymmetric with respect to the point of application of an externally applied transverse force (here R_{z_m} and R_{y_m}) and an externally applied torque (here T_m). Since the shear force expressions are satisfied at the left-hand side of the externally applied transverse forces and the torque, in order to take the effects of antisymmetry into consideration, the (-1) values are included:

$$B_{2,n1} = R_{z_m}\Bigg(EI_\xi \sum_{n=1}^{j} -k_n^3 a_n \mathrm{e}^{-k_n|L-x_m|} + EI_{v\xi} \sum_{n=1}^{j} -k_n^3 \Pi_n a_n \mathrm{e}^{-k_n|L-x_m|} - K_{tw,r} \sum_{n=1}^{j} a_n \mathrm{e}^{-k_n|L-x_m|}\Bigg),$$

$$B_{2,n2} = R_{y_m}\Bigg(EI_\xi \sum_{n=1}^{j} -k_n^3 \gamma_n c_n \mathrm{e}^{-k_n|L-x_m|} + EI_{v\xi} \sum_{n=1}^{j} -k_n^3 c_n \mathrm{e}^{-k_n|L-x_m|} - K_{tw,r} \sum_{n=1}^{j} \gamma_n c_n \mathrm{e}^{-k_n|L-x_m|}\Bigg),$$

$$B_{2,n3} = T_m\Bigg(EI_\xi \sum_{n=1}^{j} -k_n^3 \Psi_n b_n \mathrm{e}^{-k_n|L-x_m|} + EI_{v\xi} \sum_{n=1}^{j} -k_n^3 \lambda_n b_n \mathrm{e}^{-k_n|L-x_m|} - K_{tw,r} \sum_{n=1}^{j} \Psi_n b_n \mathrm{e}^{-k_n|L-x_m|}\Bigg).$$

$$B_{3,n1} = R_{z_m}\Bigg((-1)EI_v \sum_{n=1}^{j} -k_n^3 \Pi_n a_n \mathrm{e}^{-k_n|x_m|} + (-1)EI_{v\xi} \sum_{n=1}^{j} -k_n^3 a_n \mathrm{e}^{-k_n|x_m|} + K_{tv,l} \sum_{n=1}^{j} \Pi_n a_n \mathrm{e}^{-k_n|x_m|}\Bigg),$$

$$B_{3,n2} = R_{y_m}\Bigg((-1)EI_v \sum_{n=1}^{j} -k_n^3 c_n \mathrm{e}^{-k_n|x_m|} + (-1)EI_{v\xi} \sum_{n=1}^{j} -k_n^3 \gamma_n c_n \mathrm{e}^{-k_n|x_m|} + K_{tv,l} \sum_{n=1}^{j} c_n \mathrm{e}^{-k_n|x_m|}\Bigg),$$

$$B_{3,n3} = T_m\Bigg((-1)EI_v \sum_{n=1}^{j} -k_n^3 \lambda_n b_n \mathrm{e}^{-k_n|x_m|} + (-1)EI_{v\xi} \sum_{n=1}^{j} -k_n^3 \Psi_n b_n \mathrm{e}^{-k_n|x_m|} + K_{tw,l} \sum_{n=1}^{j} \lambda_n b_n \mathrm{e}^{-k_n|x_m|}\Bigg),$$

$$B_{4,n1} = R_{z_m}\Bigg(EI_v \sum_{n=1}^{j} -k_n^3 \Pi_n a_n \mathrm{e}^{-k_n|L-x_m|} + EI_{v\xi} \sum_{n=1}^{j} -k_n^3 a_n \mathrm{e}^{-k_n|L-x_m|} - K_{tv,r} \sum_{n=1}^{j} \Pi_n a_n \mathrm{e}^{-k_n|L-x_m|}\Bigg)$$

$$B_{4,n2} = R_{y_m}\Bigg(EI_v \sum_{n=1}^{j} -k_n^3 c_n \mathrm{e}^{-k_n|L-x_m|} + EI_{v\xi} \sum_{n=1}^{j} -k_n^3 \gamma_n c_n \mathrm{e}^{-k_n|L-x_m|} - K_{tv,r} \sum_{n=1}^{j} c_n \mathrm{e}^{-k_n|L-x_m|}\Bigg),$$

$$B_{4,n3} = T_m\Bigg(EI_v \sum_{n=1}^{j} -k_n^3 \lambda_n b_n \mathrm{e}^{-k_n|L-x_m|} + EI_{v\xi} \sum_{n=1}^{j} -k_n^3 \Psi_n b_n \mathrm{e}^{-k_n|L-x_m|} - K_{tw,r} \sum_{n=1}^{j} \lambda_n b_n \mathrm{e}^{-k_n|L-x_m|}\Bigg).$$

$$B_{5,n1} = R_{z_m} \sum_{n=1}^{j} k_n^2 a_n \mathrm{e}^{-k_n|x_m|}, \quad B_{5,n2} = R_{y_m} \sum_{n=1}^{j} k_n^2 \gamma_n c_n \mathrm{e}^{-k_n|x_m|}, \quad B_{5,n3} = T_m \sum_{n=1}^{j} k_n^2 \Psi_n b_n \mathrm{e}^{-k_n|x_m|}.$$

$$B_{6,n1} = R_{z_m} \sum_{n=1}^{j} k_n^2 a_n \mathrm{e}^{-k_n|L-x_m|}, \quad B_{6,n2} = R_{y_m} \sum_{n=1}^{j} k_n^2 \gamma_n c_n \mathrm{e}^{-k_n|L-x_m|}, \quad B_{6,n3} = T_m \sum_{n=1}^{j} k_n^2 \Psi_n b_n \mathrm{e}^{-k_n|L-x_m|}.$$

$$B_{7,n1} = R_{z_m} \sum_{n=1}^{j} k_n^2 \Pi_n a_n \mathrm{e}^{-k_n|x_m|}, \quad B_{7,n2} = R_{y_m} \sum_{n=1}^{j} k_n^2 c_n \mathrm{e}^{-k_n|x_m|}, \quad B_{7,n3} = T_m \sum_{n=1}^{j} k_n^2 \lambda_n b_n \mathrm{e}^{-k_n|x_m|}.$$

$$B_{8,n1} = R_{z_m} \sum_{n=1}^{j} k_n^2 \Pi_n a_n \mathrm{e}^{-k_n|L-x_m|}, \quad B_{8,n2} = R_{y_m} \sum_{n=1}^{j} k_n^2 c_n \mathrm{e}^{-k_n|L-x_m|}, \quad B_{8,n3} = T_m \sum_{n=1}^{j} k_n^2 \lambda_n b_n \mathrm{e}^{-k_n|L-x_m|}.$$

$$B_{9,n1} = R_{z_m}\Bigg((-1)GJ \sum_{n=1}^{j} -k_n \Phi_n a_n \mathrm{e}^{-k_n|x_m|} - (-1)E\Gamma_{\mathrm{O}} \sum_{n=1}^{j} -k_n^3 \Phi_n a_n \mathrm{e}^{-k_n|x_m|} - K_{tor,l} \sum_{n=1}^{j} \Phi_n a_n \mathrm{e}^{-k_n|x_m|} \Bigg),$$

$$B_{9,n2} = R_{y_m}\Bigg((-1)GJ \sum_{n=1}^{j} -k_n \sigma_n c_n \mathrm{e}^{-k_n|x_m|} - (-1)E\Gamma_{\mathrm{O}} \sum_{n=1}^{j} -k_n^3 \sigma_n c_n \mathrm{e}^{-k_n|x_m|} - K_{tor,l} \sum_{n=1}^{j} \sigma_n c_n \mathrm{e}^{-k_n|x_m|} \Bigg),$$

$$B_{9,n3} = T_m\Bigg((-1)GJ \sum_{n=1}^{j} -k_n b_n \mathrm{e}^{-k_n|x_m|} - (-1)E\Gamma_{\mathrm{O}} \sum_{n=1}^{j} -k_n^3 b_n \mathrm{e}^{-k_n|x_m|} - K_{tor,l} \sum_{n=1}^{j} b_n \mathrm{e}^{-k_n|x_m|} \Bigg).$$

$$B_{10,n1} = R_{z_m}\Bigg(GJ \sum_{n=1}^{j} -k_n \Phi_n a_n \mathrm{e}^{-k_n|L-x_m|} - E\Gamma_{\mathrm{O}} \sum_{n=1}^{j} -k_n^3 \Phi_n a_n \mathrm{e}^{-k_n|L-x_m|} + K_{tor,r} \sum_{n=1}^{j} \Phi_n a_n \mathrm{e}^{-k_n|L-x_m|} \Bigg),$$

$$B_{10,n2} = R_{y_m}\Bigg(GJ \sum_{n=1}^{j} -k_n \sigma_n c_n \mathrm{e}^{-k_n|L-x_m|} - E\Gamma_{\mathrm{O}} \sum_{n=1}^{j} -k_n^3 \sigma_n c_n \mathrm{e}^{-k_n|L-x_m|} + K_{tor,r} \sum_{n=1}^{j} \sigma_n c_n \mathrm{e}^{-k_n|L-x_m|} \Bigg),$$

$$B_{10,n3} = T_m\Bigg(GJ \sum_{n=1}^{j} -k_n b_n \mathrm{e}^{-k_n|L-x_m|} - E\Gamma_{\mathrm{O}} \sum_{n=1}^{j} -k_n^3 b_n \mathrm{e}^{-k_n|L-x_m|} + K_{tor,r} \sum_{n=1}^{j} b_n \mathrm{e}^{-k_n|L-x_m|} \Bigg).$$

$$B_{11,n1} = R_{z_m}\Bigg(\sum_{n=1}^{j} k_n^2 \Phi_n a_n \mathrm{e}^{-k_n|x_m|} \Bigg), \quad B_{11,n2} = R_{y_m}\Bigg(\sum_{n=1}^{j} k_n^2 \sigma_n c_n \mathrm{e}^{-k_n|x_m|} \Bigg),$$

$$B_{11,n3} = T_m\Bigg(\sum_{n=1}^{j} k_n^2 b_n \mathrm{e}^{-k_n|x_m|} \Bigg).$$

$$B_{12,n1} = R_{z_m}\Bigg(\sum_{n=1}^{j} k_n^2 \Phi_n a_n \mathrm{e}^{-k_n|L-x_m|} \Bigg), \quad B_{12,n2} = R_{y_m}\Bigg(\sum_{n=1}^{j} k_n^2 \sigma_n c_n \mathrm{e}^{-k_n|L-x_m|} \Bigg),$$

$$B_{12,n3} = T_m\Bigg(\sum_{n=1}^{j} k_n^2 b_n \mathrm{e}^{-k_n|L-x_m|} \Bigg). \tag{B3}$$

The following equations give the coefficients of matrix E,

$$E_{n1,n} = \mathrm{e}^{k_n x}, \quad E_{n2,n} = \Pi_n \mathrm{e}^{k_n x}, \quad E_{n3,n} = \Phi_n \mathrm{e}^{k_n x}, \tag{B4}$$

where n varies from 1 to $2j$ ($j = 6$) in each row and the row indexes $n1$, $n2$ and $n3$ are those defined in equation (B3).

Similarly, the coefficients of matrix G are given in the following set of equations

$$G_{n1,n1} = R_{z_m}\Bigg(\sum_{n=1}^{j} a_n \mathrm{e}^{-k_n|x-x_m|} + (q)(1/K_{st,w}) \Bigg),$$

$$G_{n1,n2} = R_{y_m} \sum_{n=1}^{j} \gamma_n c_n \mathrm{e}^{-k_n|x-x_m|}, \quad G_{n1,n3} = T_m \sum_{n=1}^{j} \psi_n b_n \mathrm{e}^{-k_n|x-x_m|},$$

where if $x = x_m$ then $q = 1$, otherwise $q = 0$.

In Rz_m and Ry_m and T_m the index m again varies from 1 to k. The row and the column indexes $n1$, $n2$ and $n3$ are those defined in equations (B3) and (B4):

$$G_{n2,n1} = R_{z_m} \sum_{n=1}^{j} \Pi_n a_n e^{-k_n|x-x_m|}, \quad G_{n2,n2} = R_{y_m}\left(\sum_{n=1}^{j} c_n e^{-k_n|x-x_m|} + (q)(1/K_{st,v}) \right),$$

$$G_{n2,n3} = T_m \sum_{n=1}^{j} \lambda_n b_n e^{-k_n|x-x_m|}, \quad G_{n3,n1} = R_{z_m} \sum_{n=1}^{j} \Phi_n a_n e^{-k_n|x-x_m|}.$$

$$G_{n3,n2} = R_{y_m} \sum_{n=1}^{j} \sigma_n c_n e^{-k_n|x-x_m|}, \quad G_{n3,n3} = T_m\left(\sum_{n=1}^{j} b_n e^{-k_n|x-x_m|} + (q)(1/K_{s,tor}) \right). \quad \text{(B5)}$$

The terms of the forcing vector D_{MB} are given in the following equations for the case where the torsion-bending stiffness is included in the analysis, so $j = 6$:

$$D_{MB_1} = \left((-1)EI_\xi \sum_{n=1}^{j} - k_n^3 a_n e^{-k_n|x_f|} + (-1)EI_{v\xi} \sum_{n=1}^{j} - k_n^3 \Pi_n a_n e^{-k_n|x_f|} + K_{tw,l} \sum_{n=1}^{j} a_n e^{-k_n|x_f|} \right),$$

$$D_{MB_2} = \left(EI_\xi \sum_{n=1}^{j} - k_n^3 a_n e^{-k_n|L-x_f|} + EI_{v\xi} \sum_{n=1}^{j} - k_n^3 \Pi_n a_n e^{-k_n|L-x_f|} - K_{tw,r} \sum_{n=1}^{j} a_n e^{-k_n|L-x_f|} \right),$$

$$D_{MB_3} = \left((-1)EI_v \sum_{n=1}^{j} - k_n^3 \Pi_n a_n e^{-k_n|x_f|} + (-1)EI_{v\xi} \sum_{n=1}^{j} - k_n^3 a_n e^{-k_n|x_f|} + K_{tv,l} \sum_{n=1}^{j} \Pi_n a_n e^{-k_n|x_f|} \right),$$

$$D_{MB_4} = \left(EI_v \sum_{n=1}^{j} - k_n^3 \Pi_n a_n e^{-k_n|L-x_f|} + EI_{v\xi} \sum_{n=1}^{j} - k_n^3 a_n e^{-k_n|L-x_f|} - K_{tv,r} \sum_{n=1}^{j} \Pi_n a_n e^{-k_n|L-x_f|} \right),$$

$$D_{MB_5} = \left(\sum_{n=1}^{j} k_n^2 a_n e^{-k_n|x_f|} \right), \quad D_{MB_6} = \left(\sum_{n=1}^{j} k_n^2 a_n e^{-k_n|L-x_f|} \right),$$

$$D_{MB_7} = \left(\sum_{n=1}^{j} k_n^2 \Pi_n a_n e^{-k_n|x_f|} \right), \quad D_{MB_8} = \left(\sum_{n=1}^{j} k_n^2 \Pi_n a_n e^{-k_n|L-x_f|} \right),$$

$$D_{MB_9} = \left((-1)GJ \sum_{n=1}^{j} - k_n \Phi_n a_n e^{-k_n|x_f|} - (-1)E\Gamma_O \sum_{n=1}^{j} - k_n^3 \Phi_n a_n e^{-k_n|x_f|} - K_{tor,l} \sum_{n=1}^{j} \Phi_n a_n e^{-k_n|x_f|} \right),$$

$$D_{MB_{10}} = \left(GJ \sum_{n=1}^{j} - k_n \Phi_n a_n e^{-k_n|L-x_f|} - E\Gamma_O \sum_{n=1}^{j} - k_n^3 \Phi_n a_n e^{-k_n|L-x_f|} + K_{tor,r} \sum_{n=1}^{j} \Phi_n a_n e^{-k_n|L-x_f|} \right),$$

$$D_{MB_{11}} = \left(\sum_{n=1}^{j} k_n^2 \Phi_n a_n e^{-k_n|x_f|} \right), \quad D_{MB_{12}} = \left(\sum_{n=1}^{j} k_n^2 \Phi_n a_n e^{-k_n|L-x_f|} \right),$$

$$D_{MB_{n1}} = \left(\sum_{n=1}^{j} a_n e^{-k_n|x_f-x_m|} \right), \quad D_{MB_{n2}} = \left(\sum_{n=1}^{j} \Pi_n a_n e^{-k_n|x_f-x_m|} \right),$$

$$D_{MB_{n3}} = \left(\sum_{n=1}^{j} \Phi_n a_n e^{-k_n|x_f-x_m|} \right). \quad \text{(B6)}$$

Indexes n_1, n_2 and n_3 assume the same variations as in equations (B3)–(B5). Since the shear force and the torque expressions are antisymmetric with respect to the point of application of transverse force P_z; in order to take the effects of antisymmetry into consideration, (-1) values are included in terms D_{MB1}, D_{MB3} and D_{MB9}.

If the torsion-bending stiffness is excluded from the analysis, then $j = 5$. The terms involving $E\Gamma_O$ and the terms related to the axial displacement u (i.e., ϕ') and its derivatives should appropriately be deleted from equations (B3)–(B6).

APPENDIX C: NOMENCLATURE

a_n	nth flexural displacement coefficient in z direction
b_n	nth torsional displacement coefficient
c_n	nth flexural displacement coefficient in y direction
c_y	eccentricity in y direction
c_z	eccentricity in z direction
k_n	nth wave number
m	mass per unit length of channels
t	time
u	warping displacement
v	flexural displacement in y direction
x, y, and z	spatial variables; co-ordinate system
w	flexural displacement in z direction
A	constant channel cross-sectional area
C	centroid of channels
E	Young's modulus
G	shear modulus
I_{O}	polar second moment of area about shear centre
I_v	second moment of area about v-axis
$I_{v\xi}$	product moment of area about $v\xi$-axes
I_ξ	second moment of area about ξ-axis
J	torsion constant
K_t	transverse spring
K_{tor}	torsional spring
L	total length of channels
O	shear centre of channels
P_y	transverse load in y direction
P_z	transverse load in z direction
T	resulting torque about shear centre
XL	length of each bay in periodic channels
v, ξ	centroidal axes
ϕ	torsional displacement
ρ	material density
ω	angular frequency
η_ξ, η_v, $\eta_{v\xi}$	flexural damping coefficients
η_t	torsional damping coefficient
Γ_{O}	torsion-bending constant about shear centre
i	$\sqrt{-1}$
$'$	$\partial/\partial x$
$''$	$\partial^2/\partial x^2$
$'''$	$\partial^3/\partial x^3$
$\|\ \|$	absolute value

Dummy variables confined to certain sections are clearly defined wherever applicable.